Biochimica et Biophysica Acta, 980 (1989) 1–8
Elsevier

BBA 74342

Reversible and irreversible rotating field-induced membrane modifications

G. Fuhr, T. Müller and R. Hagedorn

Department of Biology, Humboldt University of Berlin, Berlin (G.D.R.)

(Received 27 June 1988)
(Revised manuscript received 28 November 1988)

Key words: Electrorotation; Transmembrane potential; Phase difference; Membrane modification; Membrane behavior, non-linear

We analyse the charge distribution as submitted by additionally induced transmembrane potentials in rotating electric fields. In contrast to d.c. and a.c. fields, in rotating fields the induced peak potential differences across the membrane systems are phase shifted with respect both to each other and to the external field vector. These phase differences are strongly frequency-dependent but were also influenced by the electrical properties of both the cell and the surrounding medium. We extend our investigation up to the non-linear field strength range of electrorotation and found reversible and irreversible changes in the rotational behavior of several cells. The most convenient variables for describing non-linear electrorotation are the characteristic frequency (f_{c1}) and the corresponding angular velocity (ω_c) of the cells. With increasing field strength the observed rotational behavior becomes more and more irreversible and finally rupture of the membrane occurs.

Introduction

Arnold and Zimmermann [1] were the first to study the rotation of plant cells in rotating electric fields. The rotation phenomena of cells, named electrorotation, was further investigated both experimentally and theoretically [2–5], and found useful for analysing electric properties of individual cells in suspension.

Theoretical investigations have shown that the rotation measurements reflect the dielectric constants and conductivities of the cell components, especially that of the membrane systems [4,5].

The field strength applied in most experiments described in the literature ranges between 2 and 10 kV/m. In a theoretical paper [6] we calculated the rotating field-induced transmembrane potentials and found the induced peak membrane potentials to be phase shifted both with respect to each other (if more than one membrane system exists, e.g. in plant protoplasts), as well as in comparison to the rotating field vector.

Depending on the cell size, cells are able to rotate at angular velocities of more than 10 rev/s without any damage near the breakdown field strength. From a theoretical point of view we postulated that with increasing field strength non-linear field effects should be become more and more visible in the rotation spectra. In such a case the relationship between the electric polarization and the field strength must also become non-linear. According to our theoretical assumptions [3,6], non-linearities must be reflected not only in a changed dependence of the angular velocity of the cell (ω_c) on the square of the applied field strength, but also in a shift of the characteristic frequency (f_{c1}) (which usually does not depend on the field strength).

The purpose of this paper is to investigate theoretically and experimentally linear and non-linear rotational behavior in more detail. This is of practical interest, since experiments of several authors indicated that with constant and alternating fields in the non-linear range, it is possible to obtain information about the membrane structure, pore formation and modification of ion channels, as well as on pertubations of the distribution of membrane compounds [8–13]. On the other hand, for measurement of the cell properties it is obligatory to know the field strength range at which non-linear effects become dominant.

For a better understanding it is helpful to analyse the charge distribution on both sites of the membrane and the resulting transmembrane potentials before interpreting non-linear effects.

Correspondence: G. Fuhr, Department of Biology, Humboldt University of Berlin, Invalidenstrasse 42, 1040 Berlin, G.D.R.

0005-2736/89/$03.50 © 1989 Elsevier Science Publishers B.V. (Biomedical Division)

Materials and Methods

Field generation

Rotating fields were produced using square pulses [14]. Four stainless steel needles arranged as shown in Fig. 1 were used as electrodes. With this arrangement a field strength of 2–40 kV/m can be generated. The rotating field was checked by rotation of small cellulose particles, spherical in their geometry and of constant electrical properties. The field between the electrodes was found to be homogeneous (±2%) inside the marked circle (dotted line, Fig. 1B). For measurements, cells were sedimented on the bottom of the chamber, which was carefully cleaned with alcohol or consisted of a gelatin layer. The cell rotational velocity was many orders of magnitude lower than that of the driving rotating field, and the period can be easily measured using a stop-watch. To measure cells rapidly spinning at extremely high field strength we used chopped rotating fields [6] and a video system connected to the microscope. The chopper frequency varied between 10 and 100 Hz. Since a steady rate of cell rotation occurs within $< 10^{-4}$ s after switching on the electric field the chopping was without influence on the rotational behavior. Measurement of f_{c1} after switching off the external field was done using an low measuring field (< 5 kV/m) to minimize additional field effects.

The temperature was measured inside the chamber using a miniture thermo-sensor and was found to increase maximally by one degree at field strength near the electric breakdown of the membrane.

Cell preparation

Mesophyll protoplasts (*Avena sativa* L.) were prepared according to Hampp and Ziegler [15]. After isolation the protoplasts were washed twice in 0.5 M mannitol solution to reduce the external conductivity. The conductivity of the suspension was calibrated with KCl. This treatment resulted in an observed electrorotation at 25°C that was constant for several hours.

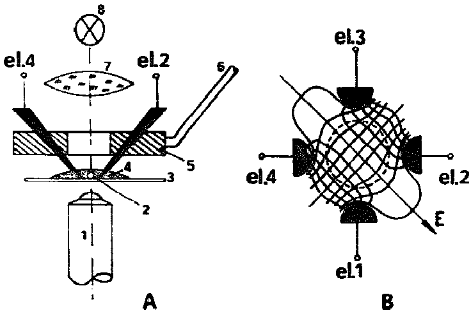

Fig. 1. Measuring chamber and electric field distribution. (A) 1, Microscope; 2, cell; 3, microscope slide; 4, cell suspension droplet; 5, electrode holder; 6, manipulator; 7, lens; 8, lamp; el. 1–4, electrodes. (B) Field and equipotential lines between the four electrodes (measured by point electrode against ground) in one of the four positions of the field vector. In our experiments the rotating field was a discontinuous one, where the field vector is changing in 90 degree steps from electrode to electrode.

Vacuoles were prepared from protoplasts (*Avena sativa* L.) either by application of short field pulses and following mechanical rupture of the plasmalemma, by short changes of the external osmolarity or by rapid changes of the external pH.

Chloroplasts (*Nicotiana plumbaginifolia*) were prepared according to Reiners and Beady [16].

Starch granules (*Solanum tuberosum* L.) were received from homogenized potatos and following washed several times in aqua dest.

Moss spores (*Plagiothecium denticulatum* L.) were also washed twice in aqua dest.

Mouse oocytes were obtained from 6–10-week-old mice (Dummerstorf strain) and released from the oviducts into Dulbecco's medium 20–25 h after human chorionic gonadotropin injection. Before measurement the cells were washed four times in 0.28 M mannitol solution and the conductivity was calibrated with $CaCl_2$ (see Ref. 17).

Results

1. Theoretical results

As recently described [6], and in contrast to d.c. and a.c. fields, rotating field induced transmembrane potentials are phase shifted with respect to the external field vector. In the case of cells consisting of more than one membrane system (e.g., plant protoplasts with a large central vacuole) the induced membrane potentials are phase shifted with respect to each other, too. Therefore, before describing the measured rotational behavior of cells as a function of the field strength we will discuss from a theoretical point of view rotating field induced membrane potentials and their phase differences to the external field vector, describing plant protoplasts by a three-shell model.

The mathematical details are discussed elsewhere [3,6].

In Fig. 2 a plant protoplast is shown in a schematic cross section in a simplified form, divided into different dielectrics corresponding to the plasmalemma (Pl), cytoplasm (Cp), tonoplast (Tp) and the vacuole interior (i). This model has proved useful for understanding the rotating field action and calculating the rotating field-induced potentials across both membrane systems as a function of the angular frequency of the field vector (Fig. 3A, B) and the phase differences at different external conductivities (Fig. 4A, B).

Fig. 3 shows that only at very high field frequencies are the induced peak membrane potentials of the

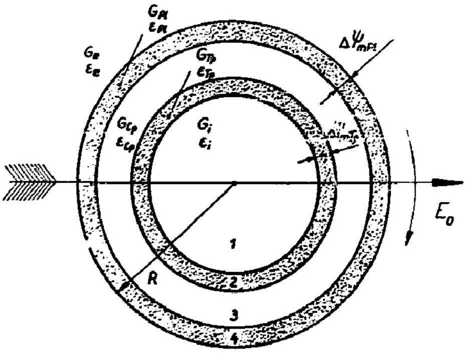

Fig. 2. Schematic cross section of a plant protoplast with large central vacuole as spherical shell model. $\Delta\psi_m$ are potential differences across the membrane, where E_o is the rotating field vector, G are the conductivities, ε are the permittivities of the corresponding media 1–4.

tonoplast and plasmalemma ($\Delta\hat{\psi}_{mPL}$; $\Delta\hat{\psi}_{mTP}$) equal (hatched areal).

The electric loading of the outer membrane decreases with increasing field frequency. This is caused by the fact that the impedance of the membrane decreases with increasing frequency due to its capacitive component. It should be noted that the resulting transmembrane potential at every point of the membrane is composed of a superposition of the constant endogenous and the induced potential difference, and consequently the membrane loading of opposite cell sides is unequal [18,19]. During positive field cycles one side of the membrane is more stressed than the other, during negative cycles the situation is exactly reversed. The average stress on the two sides is equal.

The phase difference between the peak membrane potentials of both membranes can reach nearly 75 degrees (Fig. 4A, B) and is strongly field-frequency-dependent.

For a better understanding of the theoretical results shown in Fig. 4 we have added Fig. 5. Here only the outer membrane (· · · · · ·) is interpreted in more detail. Both charge separations on the inner (———) and outer (— — —) side of the membrane are plotted and are found to be phase shifted to the external field vector too. It has to be noted that this diagram, of course, cannot reflect the absolute values of both potentials but only the phase difference (α). The absolute values $\Delta\hat{\psi}_m$ are shown in Fig. 3. But as expected from the typical rotation spectra, two extrema opposite in polarity are found in the phase difference of the charge separation on the outer side of the membrane (Fig. 5 (— — —)).

Summarizing these theoretical results it should be expected:

(i) that electric breakdown in rotating fields up to 1 MHz occurs first on the plasmalemma (see Fig. 3);

(ii) that in rotating fields a phase-shifted potential wave is moving around the cell and that at a field strength high enough to produce electrical breakdown the outer membrane is perforated in its equatorial region. At frequencies of the rotating field in the kHz-range this should lead to irreversible membrane rupture (lysis of cells).

(iii) that electrical breakdown occurs not in the direction of the external field vector, but in the direction of the phase-shifted peak potentials across the membranes.

2. *Induction of irreversible breakdown*

To test some of these conclusions we increased the external field strength at different frequencies and ex-

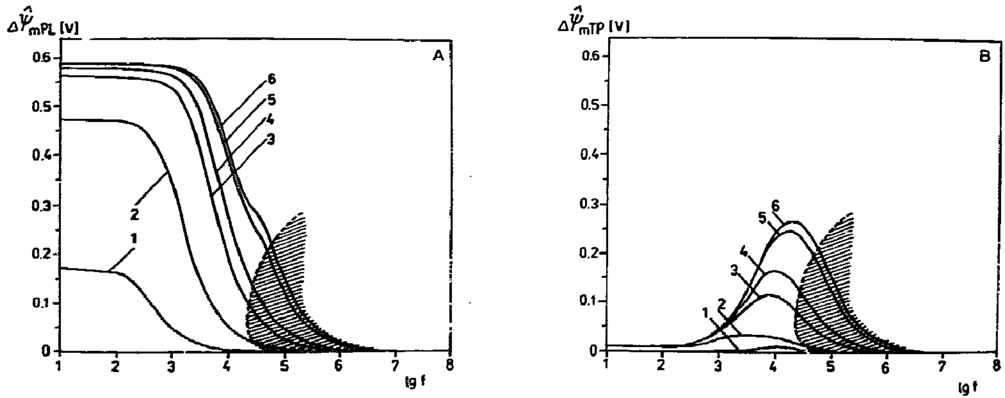

Fig. 3. Rotating field-induced peak membrane potential difference ($\Delta\hat{\psi}_m$) as a function of the frequency (f) of the rotating field (for theory, see Ref. [6]). (A) $\Delta\hat{\psi}_{mPL}$, induced peak potential difference across the plasmalemma. (B) $\Delta\hat{\psi}_{mTP}$, across the tonoplast. The hatched area in both diagrams marks the range in which $\Delta\hat{\psi}_{mPL} = \Delta\hat{\psi}_{mTP}$. The curve numbers correspond to different external conductivities. 1, $G_e = 10^{-4}$ S/m; 2, $G_e = 10^{-3}$ S/m; 3, $G_e = 5 \cdot 10^{-3}$ S/m; 4, $G_e = 10^{-2}$ S/m; 5, $G_e = 5 \cdot 10^{-2}$ S/m; 6, $G_e = 10^{-1}$ S/m. The used parameter set to calculate theoretical curves was: $G_i = 0.1$ S/m; $\varepsilon_i = 50$; $G_{Tp} = 10^{-6}$ S/m; $\varepsilon_{Tp} = 8$; $G_{Cp} = 0.1$ S/m; $\varepsilon_{Cp} = 50$; $G_{Pl} = 10^{-7}$ S/m; $\varepsilon_{Pl} = 8$; $R = 20$ μm; $\varepsilon_e = 80$; membrane thickness 4 nm; thickness of the cytoplasm 2.5 μm; field strength 20 kV/m.

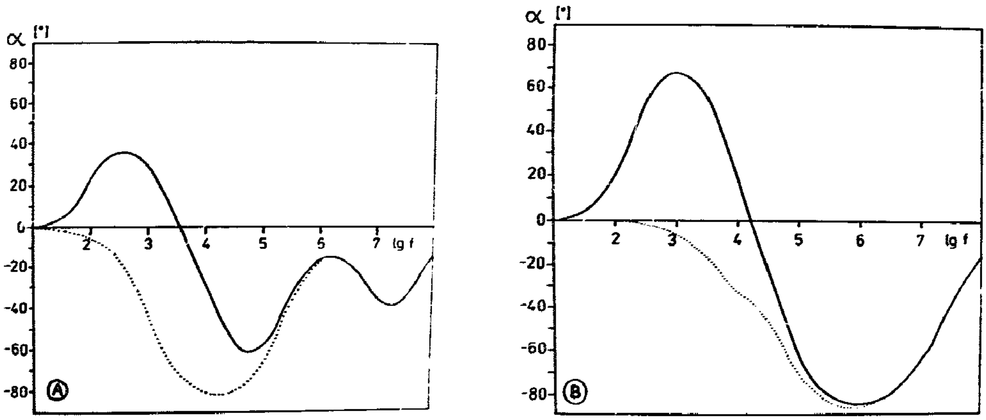

Fig. 4. Phase shift (α) of the induced peak membrane potentials ($\Delta\hat{\psi}_m$), calculated using the model of Fig. 2, as a function of the field frequency (f) at different external conductivities ((A) $G_e = 0.001$ S/m, (B) $G_e = 0.1$ S/m). ······, phase difference between $\Delta\hat{\psi}_{mPL}$ and the external field vector (E_o); ———, phase difference between $\Delta\hat{\psi}_{mTP}$ and E_o (the parameter set is identical to that of Fig. 3, for detailed calculation see Ref. 6).

ternal conductivities step by step and observed irreversible membrane rupture of protoplasts in a rotating electric field microscopically (Fig. 6).

In order to produce electrical breakdown the transmembrane potential must reach values of about 500 mV [19].

In agreement with our theoretical result represented in Fig. 3 the frequency-dependent decrease of the field-induced membrane potential must be visible by an inversely proportional increase of the external field strength, necessary for breakdown, as shown in Fig. 6. Our microscopic observations confirmed that the rupture of the plasmalemma above a critical field strength is reached without damage of the tonoplast. In all protoplast experiments but also using isolated vacuoles, the critical field strength (E_c) to induce tonoplast rupture was increased by a factor of 1.5 in comparison to the plasmalemma. This also indicates different electrical properties of both membrane systems despite of the lower radius of tonoplast.

The critical field strength can be measured very exactly using the electrorotation technique by reason of the sharp field strength value below which rotation

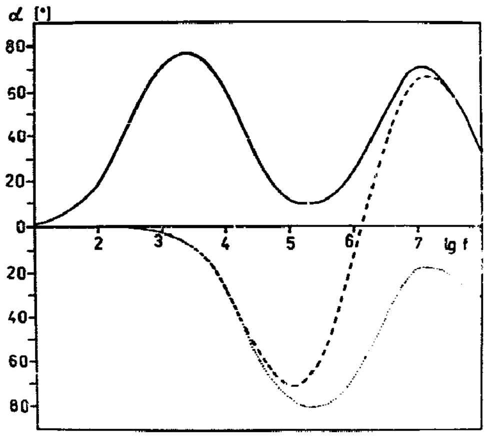

Fig. 5. Relative phase difference of the charge separations on the inner and outer side of the plasmalemma as a function of the field frequency. The field vector position is at $\alpha = 0°$ at all frequencies. — — —, maximum value of the charge separation on the outer side of the membrane; ———, maximum value of the charge separation on the inner membrane side; ······, resulting phase difference of the peak membrane potential across the plasmalemma.

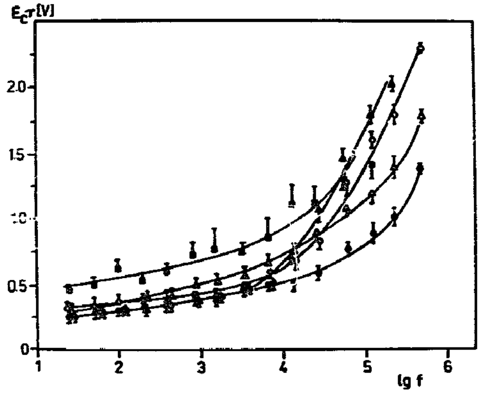

Fig. 6. Measurement of the critical field strength (E_c) of the external field, plotted as product of field strength and cell radius, at which an irreversible rupture of the membrane of protoplasts (*Avena sativa*) occurred as a function of the frequency (f). The points represent mean values of more than 10 cells, measured in 0.5 M mannitol solution and 0.5 mM $CaCl_2$ calibrated in its conductivity with KCl. Vacuoles: ■———■, $G_e = 6.7$ mS/m. Protoplasts: ▲———▲, $G_e = 1.3$ mS/m; ○———○, $G_e = 2.9$ mS/m; △———△, $G_e = 15$ mS/m; ●———●, $G_e = 44$ mS/m; r, radius of biological objects (protoplasts and vacuoles); bars, standard deviation.

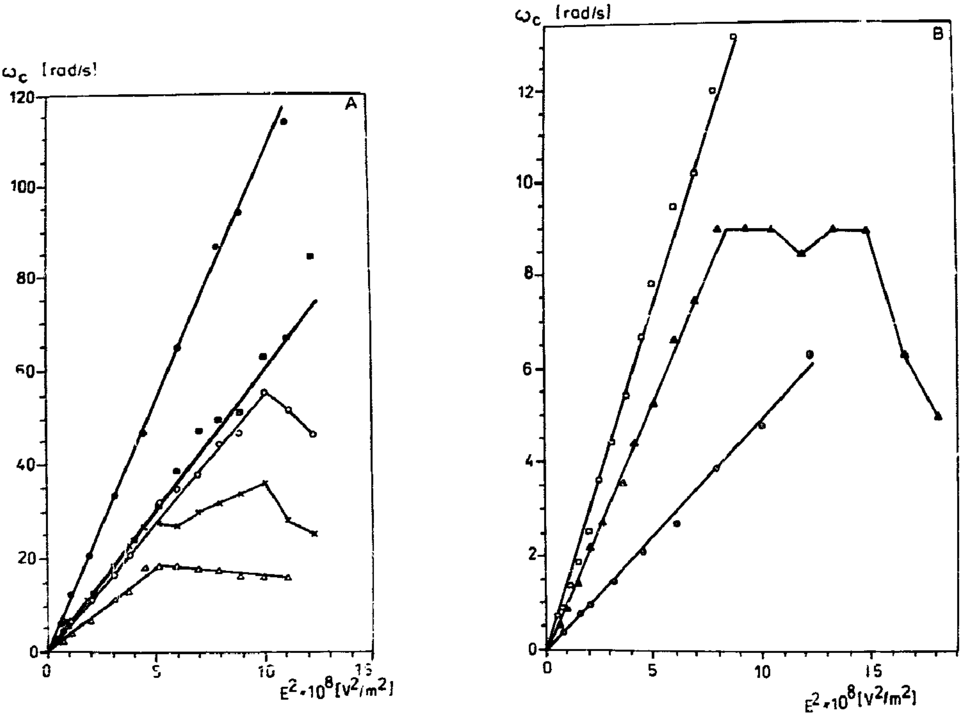

Fig. 7. Angular velocity (ω_c) of cells and cell organelles as a function of the square of the field strength (E). ●——●, moss spore ($f = 70$ kHz; $R = 9$ μm; $G_c = 2.2$ mS/m); ■——■, vacuole ($f = 8$ kHz; $R = 16.4$ μm; $G_c = 0.7$ mS/m); ○——○, protoplast ($f = 8$ kHz; $R = 20$ μm; $G_c = 1.7$ mS/m); ×——×, vacuole in 0.05% toluene ($f = 8$ kHz; $R = 20$ μm; $G_c = 0.7$ mS/m); △——△, protoplast in 20 nm gramicidin D ($f = 17$ kHz; $R = 20$ μm; $G_c = 2.3$ mS/m). □——□, chloroplast ($f = 26$ kHz; $R = 2.8$ μm; $G_c = 6.2$ mS/m); ▲——▲, isolated mouse oocyte ($f = 9$ kHz; $R = 46$ μm; $G_c = 4.2$ mS/m); ○——○, starch-granula ($f = 280$ kHz; $R = 17.2$ μm; $G_c = 4.3$ mS/m).

occurs without visible damage and above which membrane rupture occurred immediately.

Provided that the conductivity of the membrane is very much smaller than that of the cell interior and that of the suspending medium, the value of $\Delta\hat{\psi}_{mPL}$ calculated using E_c (Fig. 6) and the model (Fig. 2) is about one-half volt (0.5 V) at frequencies up to 10 kHz. This is exactly the value discussed for electrical breakdown of plasma membranes [10,12,20].

3. *Non-linear rotational behavior*

After demonstrating the capability of our calculations we can take up the non-linear rotational behavior.

In several experiments we found field strength-dependent and time-dependent changes in the angular velocity (ω_c) of cells and cell organelles (Fig. 7) below the critical field strength E_c.

In the plot shown in Fig. 7 the deviations from the straight lines are due to non-linear effects. But these deviations could arise both from a non-linear frictional or from a non-linear electromechanical behavior of the plasma membrane or cell, respectively. In order to differenciate between these possibilities we have also measured f_{c1}.

Under linear conditions f_{c1} is field strength-independent and not influenced by changes of the frictional torque (provided that the frictional conditions are changed with increasing angular velocity but are constant at a given velocity). Therefore, non-linear electrical behavior of the plasma membrane can be assumed if both the angular velocity (usually dependent on the square of the external field strength) and the characteristic frequency (usually field strength-independent) are changed in their functional dependence [3,5].

Two typical examples measuring both quantities (ω_c, f_{c1}) are shown in Fig. 8.

As recently described protoplasts freshly isolated and suspended in isotonic solution show non-linear behavior first near irreversible membrane rupture (Fig. 8A) [6], whereas osmotically stressed (plasmolysis and deplasmolysis several times) protoplasts deviate in a large field strength range from linear rotational behavior (Fig. 8B). The field strength-dependent changes of f_{c1} (Fig. 8) allows one to conclude that the measured

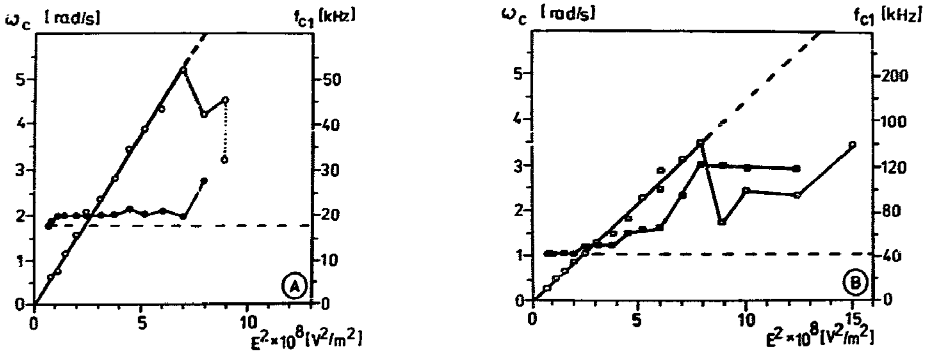

Fig. 8. Parallel measurement of both the angular velocity (ω_c) and the characteristic frequency (f_{c1}) of protoplasts as a function of the field strength (E). (A) Protoplast suspended in 0.5 M mannitol solution (G_e = 1.5 mS/m; R = 19.2 μm). (B) Protoplast after change of the external osmolarity (from 0.5 M to 0.8 M mannitol solution, G_e = 2.7 mS/m; R = 17 μm). Open symbols, ω_c; closed symbols, f_{c1}.

effects are produced by electromechanical stresses in the membrane and not by changing the frictional conditions.

4. *Reversible and irreversible changes of the rotational behavior*

From this result the question arises as to the manner in which the induced-field effects are irreversible or reversible. Such time-dependent changes at a given field strength are visible both on the angular velocity of the cell and the characteristic frequency (Fig. 9).

Note that the characteristic frequency was measured using the compensation technique according to Arnold et al. [21], that means by zero compensation of the angular velocity applying two rotating fields opposite in their spin direction and with the frequencies f and $f/4$. Therefore, parallel measurement of ω_c and f_{c1} is not possible and the curves shown in Figs. 9A and B are experimental data of two different but representative single protoplasts.

Fig. 9A indicates that at low field strength only small changes of the characteristic frequency are measurable, which are completely reversible in a very short time (ms range). With increasing field strength more and more irreversible effects become dominant and lead to a continuous increase of f_{c1} related to changes of the electrical membrane properties (relative permittivity and conductivity).

We observed different time constants describing the effect caused by switching on and off the external field (measurement after switching off the field; see Materials and Methods).

In the range where the first irreversible changes are visible, the time constant of the reversible part of the process (in all cases a nearly exponential time course) after switching off the external field varied between 10 s

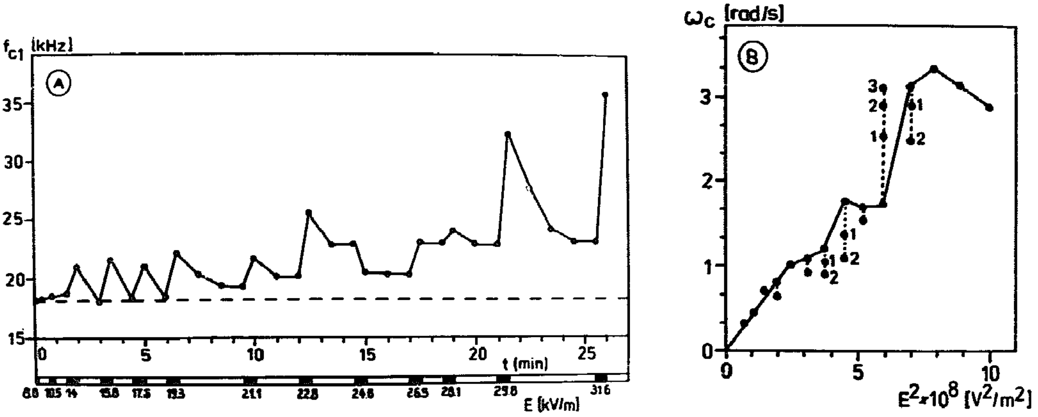

Fig. 9. (A) Time-dependent changes of the characteristic frequency (f_{c1}) of a single protoplast after switching on (■) and off (□) the external field at increasing external field strength. (B) Angular velocity (ω_c) in dependence on the field strength (E). The dotted lines and numbered points represents measurements each after 10 seconds at the same field strength.

and 1 min. The changes after switching on the field were much faster. The same results were obtained when measuring the angular velocity of cells (Fig. 9B). Therefore, there is no doubt that the described changes in the rotational behavior of protoplasts are field-mediated processes no interfering with frictional effects.

Analoguous non-linear rotational effects were investigated on mouse oocytes and zygotes, as well as suspension cultured single cells, but not for small particles. This is understandable since for small particles field strengths higher than those used are necessary to produce non-linear effects.

Thermal effects, such as heating of the cell suspension, we can exclude, since during the measuring time the temperature inside the chamber increases maximally by 1 degree.

Discussion

Our aim was to demonstrate the close connection between rotating electric field-induced charge distributions on the membrane surfaces and non-linear electrorotational behavior of cells. The most convenient variables for describing the field strength-dependent processes are the characteristic frequency (f_{c1}) and the angular velocity (ω_c) of the cell [3,5,7].

The phase-shifted peak transmembrane potentials in rotating fields improve the possibility of selectively influencing particular membranes by combining rotating fields with additional short electric pulses, which produce no phase difference between the inner or outer membrane, respectively [6].

The existence of phase-shifted potentials occurs only in rotating electric fields. Up to now in our theoretical investigations a maximum phase difference between inner and outer membrane systems of 80 degrees was not exceeded, but detailed calculations varying the membrane conductivities are necessary to formulate a general statement.

High field-strength-induced deviations of the usual electrical behavior of cells in constant and alternating electric fields are referred to in a large number of publications (see, for example, Refs. 8–13, 22, 27). Electromechanical stresses produced in the membrane by applied fields are calculated carefully by Bryant and Wolfe [8] and the distribution of tension and deformation of the membrane using ideal membrane compositions are discussed there in detail.

For real membrane systems several authors indicated that in the non-linear range of the membrane behavior, information can be obtained about the membrane structure [11–13].

From the physical point of view in the linear range the polarization (P) of the particle is usually proportional to the dielectric susceptibility (χ) and the external field strength (E). In case of non-linear electrical behavior the dielectric susceptibility becomes field strength-dependent itself. In other words, the conductivity and/or dielectric constant of the appropriate dielectrics (in our case the membranes) are no longer constants but change with increasing field strength too. This can be caused by several processes of more or less reversible character such as membrane compression and lateral tension, macromolecular orientation, pore enlargement or ion and volume flux changes [8].

Mechanical stresses in the membrane lead to elastic, and at high stresses to plastic, deformations [8,22]. This, however, is reflected in reversible and irreversible changes of the rotational behavior of the cells.

It seems to be unrealistic to hope to interpret molecular membrane modifications using the electrorotation alone. In every case additional information obtained from other experiments is necessary to differentiate the superimposed processes. Of course, it is obligatory to investigate the time course of the field-induced membrane changes after switching on and off the electric field.

In our recent paper [6] we presented experimental results which show only a small non-linear range at field strength near electrical breakdown. The cells used were protoplasts isolated from leaves of *Kalanchoe daigremontiana*. The present experiments with protoplasts isolated from mesophyll tissue of *Avena sativa* (Fig. 8A) confirm this finding.

After osmotic stress or application of ionophores or membrane-active substances the situation is completely changed (Fig. 8B). As shown by Gordon-Kamm and Steponkus [23] plasmolysis and deplasmolysis of protoplasts is coupled with membrane vesicle formation and fusion, respectively. During and after this processes the electrical membrane properties are changed [24,25]. Usually the membrane conductivity increases since the plasmolysis-deplasmolysis procedure is repeated several times and the membrane destruction and recombination processes lose their reversibility [24–26].

On the other hand, from earlier investigations we know that freshly isolated intact protoplasts of *Avena sativa* show plasmalemma conductivities of less than 10^{-7} S/m [3]. Our recent interpretation was that increasing or decreasing of the membrane conductivity below 10^{-7} S/m is not detectable in the rotational behavior. To understand better this limitation of the electrorotation technique the calculated characteristic frequency (f_{c1}) as a function of the membrane conductivity (G_m) is shown in Fig. 10.

Fig. 10 illustrates that the membrane conductivity influences the rotational behavior only in the hatched ranges (a–d). At best (at external conductivities of 10^{-4} S/m, that means the electrolyte content of distilled water) a membrane conductivity higher than 10^{-7} S/m can be determined from changes of the characteristic

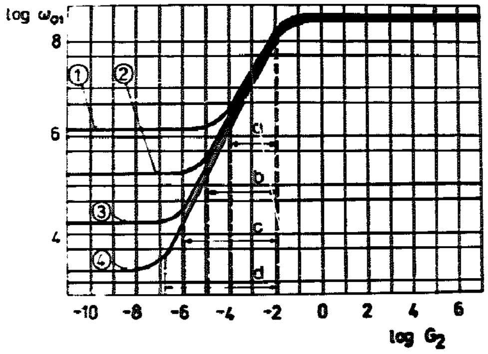

Fig. 10. Dependence of the characteristic angular velocity ($\omega_{01} = 2 \cdot \pi \cdot f_{c1}$) on the membrane conductivity (G_2) at different conductivities of the external solution (G_c). a, b, c, d, ranges in which changes of the membrane conductivity are visible in changes of the cell rotation spectra. 1, $G_e = 10^{-1}$ S/m, 2, $G_e = 10^{-2}$ S/m; 3, $G_3 = 10^{-3}$ S/m; 4, $G_e = 10^{-4}$ S/m.

frequency. At higher external conductivities the usable measuring interval is further reduced.

Our experiments were done at external conductivities near 10^{-3} S/m, therefore it seems to be understandable that changes of the membrane parameters over one order of magnitude are without effect on the rotational behavior, provided the membrane conductivity was as small as assumed above.

Summarizing the content of this paper, the electrorotation was shown to be useful in analysing both linear and non-linear rotational effects. Despite the fact that non-linear electrical behavior of cells is difficult to interpret the usuable field-strength range is large enough to analyse this effect carefully in detail. Naturally the measured non-linear rotational behavior is the result of superimposed processes of both reversible and irreversible nature. The field-strength range, as well as the changes in the rotation spectra correspond to measurements done by other field-mediated techniques and data in the literature [8,20]. It was shown that the usually applied fields, in principle, do not produce irreversible alterations of the cells [1,3], but in every case additional transmembrane potential waves are moving around the cells. Practical use of this phase-shifted potential drops are not checked up to now in detail.

However, the experimental set up to extent the electrorotation up to the non-linear range requires no special conditions. For cells with diameters between 10 and 100 μm, a field strength up to 40 kV/m is necessary (which can be easily produced by four electrodes when the distance between the opposite electrodes is smaller than 500 μm).

On the other hand, high field strength rotating fields can be used also to modify biomembranes as described in the literature for the application of d.c. and a.c. electric fields. However, detailed investigations are necessary to clearify the limitations and capabilities of rotating fields in comparison to alternating or electrostatic fields.

Acknowledgements

We thank Dipl. Biol. F. Geißler for careful preparation of mouse eggs, Dr. D.B. Kell for helpful discussion, Dr. J. Gimsa for the figure showing the equipotential lines inside the chamber and Dipl. Biol. W. Heß for chloroplast isolation.

References

1 Arnold, W.M. and Zimmermann, U. (1982) Z. Naturforsch. 37c, 908–915.
2 Hagedorn, R. and Fuhr, G. (1984) Stud. Biophys. 102, 229–238.
3 Fuhr, G. (1985) Dissertation, Humboldt-University, Berlin.
4 Sauer, F.A. and Schlögl, R.W. (1985) in Interactions between Electromagnetic Fields and Cells (Chiabrera, A., Nicolini, C. and Schwan, H.P., eds.), pp. 203–252, Plenum Press, New York.
5 Fuhr, G., Glaser, R. and Hagedorn, R. (1986) Biophys. J. 49, 395–404.
6 Fuhr, G., Hagedorn, R., Glaser, R., Gimsa, J. and Müller, T. (1987) J. Bioelectr. 6, 49–69.
7 Müller, T., Fuhr, G., Hagedorn, R. and Göring, H. (1986) Stud. Biophys. 113, 203–211.
8 Bryant, G. and Wolfe, J. (1987) J. Membr. Biol. 96, 129–139.
9 Lew, H.S. (1970) J. Biomech. 3, 569–583.
10 Benz, R. and Zimmermann, U. (1980) Bioelectrochem. Bioenerg. 7, 723–739.
11 Stulen, G. (1981) Biochim. Biophys. Acta 640, 621–627.
12 Chernomordik, L.V., Sukharev, S.I., Abidor, I.G. and Chizmadzhev, Y.A., (1983) Biochim. Biophys. Acta 736, 203–213.
13 Serpersu, E.H., Kinosita, K., Jr. and Tsong, T.Y. (1985) Biochim. Biophys. Acta 812, 779–785.
14 Fuhr, G., Hagedorn, R. and Göring, H. (1984) Stud. Biophys. 102, 221–227.
15 Hampp, R. and Ziegler, H. (1980) Planta 147, 485–494.
16 Reiners, A. and Beady, R.N. (1985) Plant Mol. Biol. 6, 291–301.
17 Fuhr, G., Geißler, F., Müller, T., Hagedorn, R. and Torner, H. (1987) Biochim. Biophys. Acta 930, 65–71.
18 Mehrle, W., Zimmermann, U. and Hampp, R. (1985) FEBS Lett. 185, 89–94.
19 Zimmermann, U. (1986) Rev. Physiol. Biochem. Pharmacol. 105, 176–256.
20 Abidor, I.G., Arakelyan, V.B., Chernomordik, Y.A., Pastushenko, V.F. and Tarasevich, M.R. (1974) Bioelectrochem. Bioenerg. 6, 37–52.
21 Arnold, W.M. and Zimmermann, U. (1983) Patent Application, official designation P 3325 843.0, received at the Patent Office, F.R.G. July 18.
22 Sackmann, E., Engelhardt, J., Fricke, K. and Gaub, H. (1984) Colloids Surf. 10, 321–335.
23 Gordon-Kamm, W.J. and Steponkus, P.L. (1984) Protoplasma 123, 83–94.
24 Wolfe, J., Dowgert, M.F. and Steponkus, P.L. (1986) J. Membr. Biol. 93, 63–74.
25 Wolfe, J., Dowgert, M.F. and Steponkus, P.L. (1985) J. Membr. Biol. 86, 127–138.
26 Wolfe, J. and Steponkus, P.L. (1981) Biochim. Biophys. Acta 643, 663–668.